

## X-Ray Scattering Study of the Magnetic Structure near the (001) Surface of $\text{UO}_2$

G. M. Watson,<sup>1</sup> Doon Gibbs,<sup>1</sup> G. H. Lander,<sup>2</sup> B. D. Gaulin,<sup>3</sup> L. E. Berman,<sup>4</sup> Hj. Matzke,<sup>2</sup> and W. Ellis<sup>5</sup>

<sup>1</sup>Physics Department, Brookhaven National Laboratory, Upton, New York 11973-5000

<sup>2</sup>European Commission, Joint Research Center, Institute for Transuranium Elements, Postfach 2340, D-76125 Karlsruhe, Germany

<sup>3</sup>Department of Physics and Astronomy, McMaster University, Hamilton, Ontario, Canada L8S 4M1

<sup>4</sup>National Synchrotron Light Source, Brookhaven National Laboratory, Upton, New York 11973-5000

<sup>5</sup>Los Alamos National Laboratory, Los Alamos, New Mexico 87545

(Received 19 March 1996)

We report glancing-incidence x-ray scattering studies of the magnetic structure observed near the (001) surface of the antiferromagnet  $\text{UO}_2$ . Within about 50 Å of the surface, the magnetic scattering intensity decreases continuously as the bulk Néel temperature is approached from below. This contrasts with the bulk transition, which is discontinuous. [S0031-9007(96)00670-9]

PACS numbers: 75.50.Ee, 75.25.+z, 75.30.Kz, 75.30.Pd

In the last several years, there have been continuing efforts to probe long ranged magnetic order at surfaces by x-ray and neutron diffraction [1–6], following many earlier studies by low energy electron diffraction [7]. The main motivation has been to discover how bulk magnetic structures are modified near a surface, where the crystal symmetry is broken. In this paper, we report synchrotron-based x-ray scattering studies of magnetic ordering near the (001) surface of the type I antiferromagnet  $\text{UO}_2$ . Our aim in choosing  $\text{UO}_2$  was twofold: first, to take advantage of its chemical inertness, which simplifies the preparation and handling of the surface; and second, to take advantage of the large resonant enhancements of the magnetic cross section which occur when the incident photon energy is tuned near the uranium  $M_{IV}$  absorption edge [8]. We have found that it is possible to observe x-ray magnetic scattering from  $\text{UO}_2$  surfaces at glancing incident angles [6], near the critical angle for total external reflection, with counting rates as high as 200/sec on a wiggler beam line. This has allowed characterization of the momentum transfer dependence of several magnetic (and charge) truncation rods along the surface normal. By tuning the incident x-ray energy through the  $M_{IV}$  edge, we have verified that the observed scattering is magnetic, and extracted forms for the variation of  $f'$  and  $f''$  with x-ray energy. A most interesting result is that within about 50 Å of the surface, the temperature dependence of the magnetic scattering intensity decreases continuously near the Néel temperature  $T_N = 30.2$  K and is well described by a power law in reduced temperature. In contrast, the bulk magnetic order parameter is well known to be discontinuous [9].

The present experiments were performed at beam lines X22C and X25 at the National Synchrotron Light Source. In both cases, double crystal monochromators [Ge and Si (111), respectively] were used to tune the incident x-ray energy to the U  $M_{IV}$  absorption edge at 3.728 keV. The sample was cut and mechanically polished to produce a surface with an (001) orientation. In order to remove the

surface damage and ensure the stoichiometry, the sample was annealed in an Ar/ $\text{H}_2$  atmosphere at 1400 °C. It then was loaded in a He-filled can and mounted on the end of a standard helium displacer refrigerator. No additional steps were taken to preserve the oxide surface layer. As determined by specular x-ray reflectivity, this surface was found to be nearly flat over the 1000 Å x-ray resolution length employed in these experiments. The bulk mosaic was 0.05°.

$\text{UO}_2$  has the face-centered cubic fluorite structure with a lattice constant of 5.47 Å at 300 K. The allowed chemical Bragg reflections are defined by  $H$ ,  $K$ , and  $L$  either all even or all odd. The diffraction pattern of a crystal supporting a surface is characterized by rods of scattering (called truncation rods) which pass through the allowed bulk Bragg points and are parallel to the surface normal [see Fig. 1(a)]. The variation of the x-ray intensity along the chemical truncation rods is determined by the decay of the electronic charge density near the surface [10]. The bulk magnetic structure of  $\text{UO}_2$  is triple  $Q$ , consisting of ferromagnetic (001)-type planes stacked antiferromagnetically along each of the  $\langle 001 \rangle$  directions. The magnetic bulk reflections are obtained by adding a  $\langle 001 \rangle$  wave vector to each allowed chemical Bragg wave vector [see Fig. 1(a)]. We may similarly define magnetic truncation rods [4], which pass through the bulk magnetic reflections, and whose intensity variation depends on the decay of the magnetization density near the surface. For an antiferromagnet, this leads both to magnetic contributions to the chemical rods as well as to the existence of pure magnetic truncation rods when  $H$  and  $K$  are mixed [see Fig. 1(a)]. The primary aim of the present experiments was to observe the (01L) magnetic rod.

The scattering geometry is illustrated in Fig. 1(b). Most of the experiments were carried out at glancing incidence, where the incident and exit angles of the x-ray beam to the surface are near the critical angle  $\alpha_c \sim 0.75^\circ$  for total external reflection. Near  $\alpha_c$ , the refraction effects

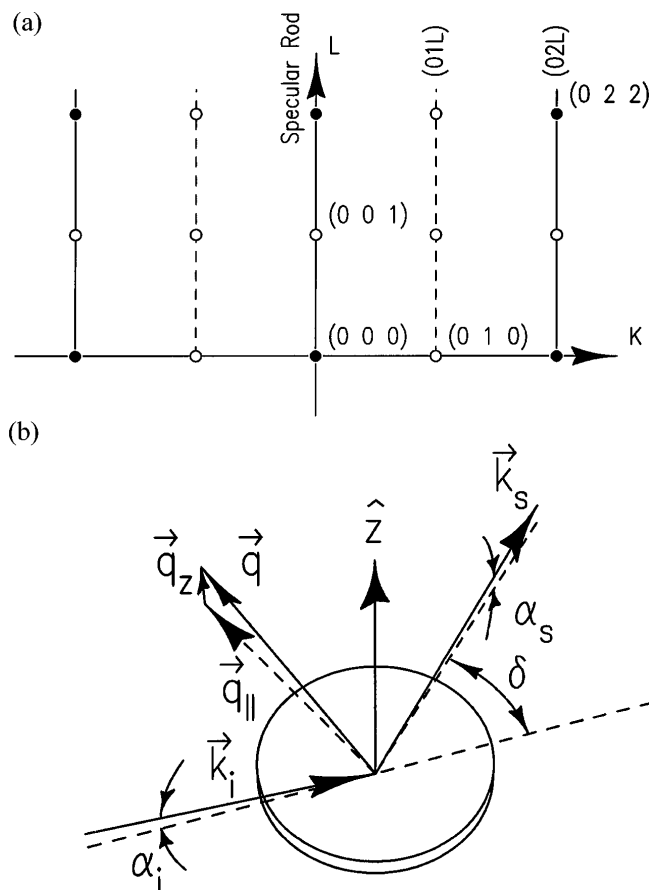


FIG. 1. (a) Reciprocal space map for the  $\text{UO}_2$  (001) surface showing chemical (solid circles) and magnetic (open circles) bulk Bragg reflections and mixed (solid lines) and magnetic (dashed lines) truncation rods. (b) Glancing-incidence scattering geometry.  $\hat{z}$  is the surface normal direction,  $\vec{k}_i$ ,  $\vec{k}_s$ , and  $\vec{q}$  are the incident, scattered, and transferred wave vectors, respectively.  $\vec{q}_z$  is the component of the momentum transfer normal to the surface.

become important and lead to an enhancement of the transmitted beam. These effects are well understood [10] and illustrated in the top of Fig. 2(a) where the intensity dependence of the  $(0\bar{2}L)$  charge scattering rod is shown. The intensity along the rod may be described by

$$I(k_i, k_s)/I_0 = (1/A_0) |T(\alpha_i)|^2 |T(\alpha_s)|^2 \left( \frac{d\sigma}{d\Omega} \right), \quad (1)$$

where  $A_0$  and  $I_0$  are the area and flux of the incident beam and  $T(\alpha)$  is the usual Fresnel transmission amplitude for x rays at an angle  $\alpha$  to the surface.  $d\sigma/d\Omega$  is the cross section for x-ray scattering and depends on the Fourier transform of the electronic charge density. Near the critical angle, the transmission coefficients exhibit maxima which lead to the peak observed in Fig. 2(a).

The lower curves in Fig. 2(a) show the intensity dependence of the pure magnetic scattering along the  $(01L)$  rod, obtained as a function of incident photon energy. Their shapes are all qualitatively similar to that of the charge

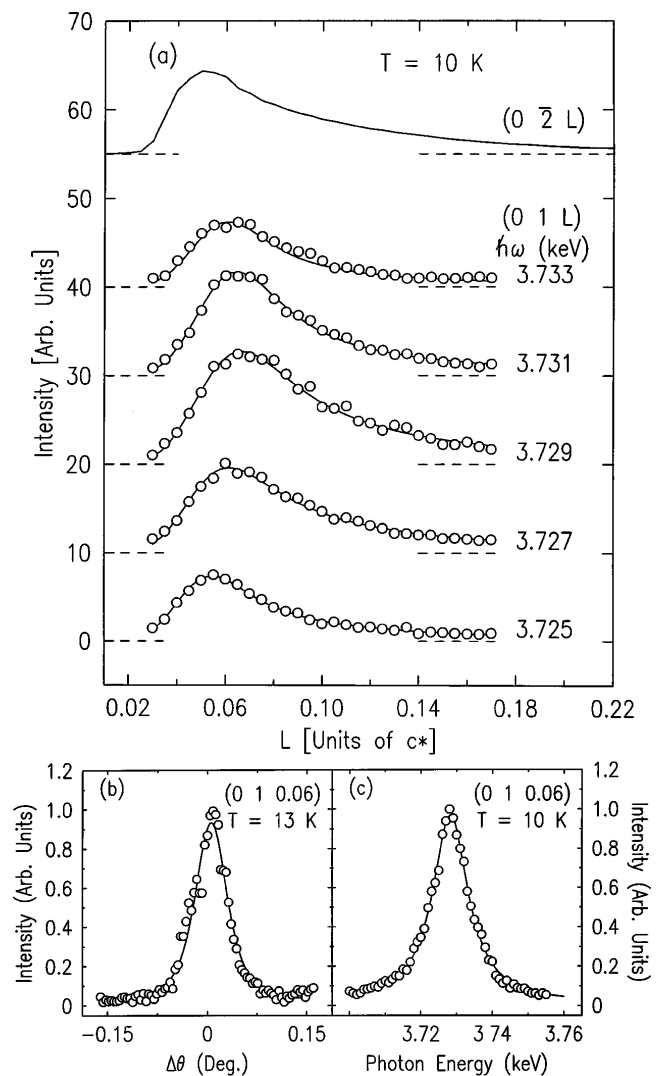


FIG. 2. Intensity of the  $(0\bar{2}L)$  charge (solid line), and  $(01L)$  magnetic (open points) truncation rods as a function of  $L$ . The magnetic rod was obtained at five photon energies. The  $(0\bar{2}L)$  rod was obtained with an incident photon energy of 3.728 keV. (b) Rocking curve of the magnetic truncation rod at  $L = 0.06$ . (c) Energy dependence of the intensity of the magnetic truncation rod at  $L = 0.06$ .

scattering. Rocking curves taken through the magnetic rod at  $L = 0.06$  [see Fig. 2(b)] give full widths of  $0.06^\circ$ , identical to that of the charge scattering rod, and close to the bulk mosaic. No variation in rocking width was observed along the rods. All of this indicates that the in-plane magnetic structure near the surface is well ordered at 10 K. The energy dependence of the magnetic intensity at fixed  $L$  is summarized in Fig. 2(c). The observed resonance is identical to that obtained in other uranium compounds and shows that the observed scattering is magnetic in origin.

Although the line shapes of the magnetic truncation rods are similar, exhibiting maxima near  $\alpha_c$  (which corresponds to  $L \sim 0.06$ ), the observed values of  $\alpha_c$  vary

as a function of photon energy. This variation arises because the critical angle depends directly on  $f'$ , which changes dramatically near an absorption edge. More precisely,  $\alpha_c^2 \sim (Z + f')\rho\lambda$ , where  $Z$  is the total charge,  $\rho$  is the average atomic density,  $\lambda$  is the wavelength, and  $f'$  is the dispersive part of x-ray amplitude. In order to model these effects versus momentum transfer and energy, we have written the magnetic scattering from a surface as

$$\left(\frac{d\sigma}{d\Omega}\right) = (A/\sin\alpha_i \sin\alpha_s) \left| \sum_{n=0}^{\infty} F^M(k_i, k_s, \hbar\omega, \hat{\epsilon}_i, \hat{\epsilon}_s, \hat{J}) \times \rho_n^M(q_{\parallel}) e^{iq_z z_n} \right|^2, \quad (2)$$

where  $A$  is the illuminated surface area,  $z_n$  is the position of the  $n$ th layer, and  $\rho_n^M$  is the amplitude of the magnetic density wave in the  $n$ th layer with wave vector  $q_{\parallel}$ . The factor  $F^M$  contains the resonant terms and depends on the incident photon energy, the polarization of the incident and scattered x rays, the incident and scattered photon wave vectors, and the direction of the magnetic moment  $\hat{J}$ . The cross section was evaluated within the distorted-wave Born approximation [11] and inserted into Eq. (1). We fitted the data by varying the anomalous corrections to the atomic form factor for uranium  $f'$  and  $f''$ , as they enter through the Fresnel coefficients  $T(\alpha_i/\alpha_s)$ , but including a separate normalization factor to account for the energy dependence of the resonant cross section. In the fitting, we convoluted the theoretical cross section with the resolution function, accounted for the surface miscut ( $\sim 0.25^\circ$ ), and added a thin attenuating overlayer to account for impurities in the He exchange gas which we believe condense on the sample surface. In addition, we have assumed that the magnetic structure is bulk truncated and that  $F^M$  is constant over the range probed in  $L$ . The resulting fits [solid lines in Fig. 2(a)] are excellent, capturing both the  $L$  dependence of the line shapes and the shift in position of the critical angle. As a check on our procedures, we have independently extracted  $f'$  and  $f''$  from measurements of the energy dependence of the specular reflectivity [12], as well as from the energy dependence of the position of the (110) Bragg reflection, in both cases as a function of photon energy. The collected results for  $f'$  are compared in Fig. 3, together with the predictions of a damped harmonic oscillator model (solid line) and the theory of Cramer and Lieberman (dashed line). The results are reassuringly self-consistent.

We turn next to the temperature dependence of the magnetic scattering. Figure 4 shows the intensity plotted versus temperature as obtained at two positions along the magnetic truncation rod, (0, 1, 0.075) and (0, 1, 0.15), and at the bulk (001) reflection. From the measured dispersion corrections to the atomic form factors, it may be shown that these values of  $(HKL)$  correspond to penetration depths of  $\sim 50$ ,  $\sim 120$ , and  $\sim 850$  Å, respectively.

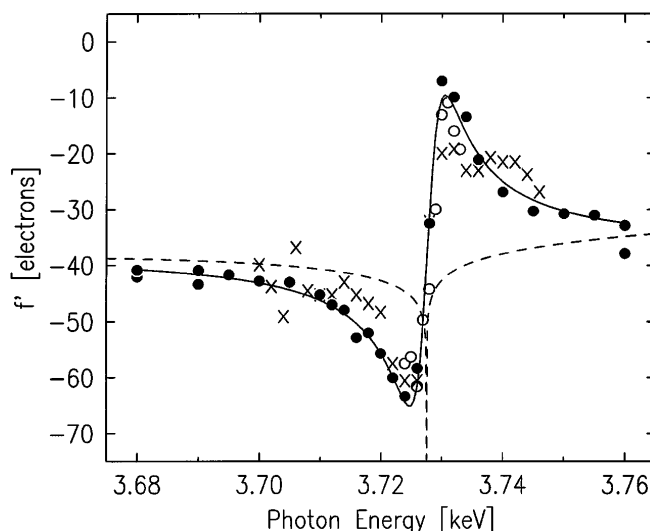


FIG. 3. Energy dependence of the real part of the anomalous dispersion correction from fits to data shown in Fig. 2(a) (open circles), from specular reflectivity measurements (solid circles) and from the shift in the position of the (110) magnetic bulk Bragg reflection (crosses). The solid line is a fit of the specular reflectivity data to a damped-harmonic oscillator model; the dashed line is the Cromer-Lieberman prediction for U. The deviation from the theory of Cromer and Lieberman is due to the strong white line present in the absorption spectrum of  $\text{UO}_2$ .

The temperature dependence of the magnetic scattering at the (001) reflection exhibits the discontinuity at  $T_N$  expected from previous studies [9]. In contrast, the magnetic scattering intensities obtained on the truncation rod fall more slowly to zero as  $T_N$  is approached from below. Indeed, they appear continuous. It is worth noting that the width of the magnetic truncation rods are temperature independent and, to within  $\pm 0.5$  K, the bulk and near surface ordering temperatures are equal. These results suggest that the magnetic structure *begins* to disorder at lower temperatures near the surface than in the bulk. This conclusion is similar to that obtained by Dosch and co-workers in their x-ray structural studies of the order-disorder transition in  $\text{Cu}_3\text{Au}$  [13]. In those experiments, the near-surface superlattice peak of the ordered alloy was found to decay continuously near  $T_0$  (the order-disorder temperature), whereas the bulk behavior was discontinuous. They interpreted their results in terms of surface-induced disordering, wherein a partially disordered layer of crystalline phase wets the near-surface volume below  $T_0$  and grows logarithmically in thickness as  $T$  approaches  $T_0$ . Surface-induced disorder was introduced for first-order transitions by Lipowsky [14] and has been discussed in many contexts since (see [15], and references therein.) Within Landau theory, these calculations yield regions of the phase diagram for which the order parameter at the surface is predicted to follow a power law in reduced temperature.

Motivated by these ideas, we have attempted a similar analysis in  $\text{UO}_2$ . Fits of the magnetic scattering intensity to a power law in reduced temperature,  $I = At^{2S}$ , where

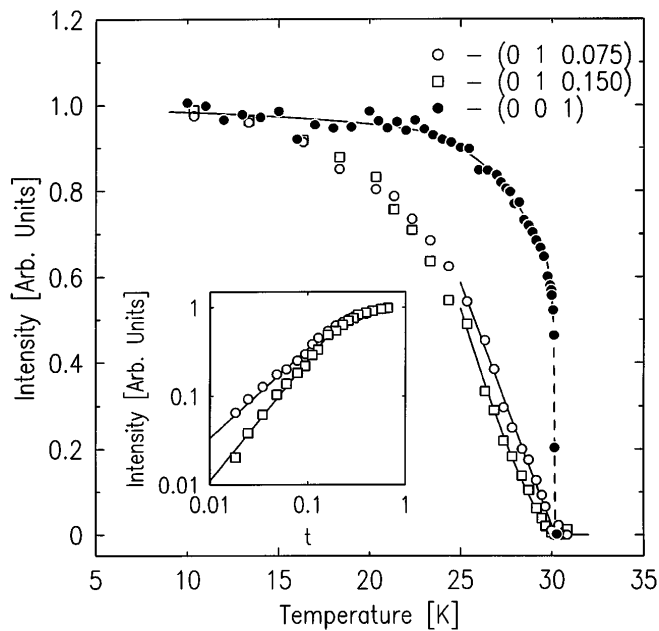


FIG. 4. Magnetic intensities obtained at the (001) specular Bragg reflection (solid circles) and along the (01L) magnetic truncation rod at  $L = 0.075$  (open circles) and 0.15 (open squares). They have been normalized to 1.0 at low temperatures. The solid lines represent best fits to a power law dependence on reduced temperature. The solid line for the (001) reflection is a guide for the eye. Inset: Log-log plot of the magnetic scattering intensity at (0, 1, 0.075) and (0, 1, 0.15) vs reduced temperature.

$t = (T_N - T)/T_N$ , are shown for two values of  $L$  by the solid lines in Fig. 4. The fits are clearly satisfactory and yield exponents  $S = 0.5 \pm 0.1$  at  $L = 0.075$  and  $S = 0.7 \pm 0.15$  at  $L = 0.150$ . Evidently, the exponents exhibit an  $L$  dependence, increasing for increasing  $\delta L$  ( $\delta L$  referred to the nearest Bragg peak), which differs from trends observed in  $\text{Cu}_3\text{Au}$  and from the predictions of Lipowsky's theory. More sophisticated models, for example, including a temperature-dependent width to the interface between the ordered and disordered magnetic regions [16], have not resolved this distinction. In this regard, it is important to note that the intensity measured along a truncation rod depends on the order parameter profile along the surface normal and reduces to the square of the average order parameter only when the atomic planes scatter in phase. Thus while our results are qualitatively consistent with the ideas of surface-induced disordering, a quantitative description of  $\text{UO}_2$  remains lacking. A fuller discussion of our analysis will be presented elsewhere [17].

We conclude by noting that we have successfully observed x-ray magnetic scattering from a pure magnetic truncation rod in  $\text{UO}_2$ . The counting rates are large enough to merit further experiments, for example, to attempt to observe the interference between the magnetic and charge lattices (which presumably differ near  $T_N$ ) in the specular reflectivity. Further improvements are possible by the

adaptation of our UHV chamber to low temperature x-ray scattering studies. From our experiments, it seems likely that the use of third generation synchrotron sources will make studies of actinide surface magnetism straightforward and may make possible studies of surface magnetism in a wider class of materials [18]. In this regard, it will be especially important to characterize the momentum transfer and temperature dependence of the magnetic surface rods at larger  $L$  than has been possible here. Experiments on these and related surfaces are continuing.

During completion of our manuscript, S. Ferrer kindly sent us a copy of his manuscript describing x-ray magnetic scattering experiments on  $\text{Co}_3\text{Pt}$  surfaces [17] which we gratefully acknowledge. We thank V. Meyritz for assistance in the sample preparation. Work performed at Brookhaven is supported by the U.S. DOE under Contract No. DE-AC02-CH7600016. B. D. G. acknowledges financial support from NSERC of Canada, OCMR of Ontario, and the Alfred P. Sloan Foundation.

- [1] G. P. Flecher *et al.*, Phys. Rev. Lett. **52**, 1539 (1984).
- [2] K. Al Usta *et al.*, Physica (Amsterdam) **173B**, 65 (1991).
- [3] C.-C. Kao *et al.*, Phys. Rev. Lett. **65**, 373 (1990).
- [4] A. Fasolino *et al.*, Phys. Rev. B **47**, 3877 (1993).
- [5] N. Bernhoeft *et al.*, J. Magn. Magn. Mater. **140**, 1421 (1995); A. Stunault, S. Langridge, C. Vettier, D. Gibbs, and N. Bernhoeft (unpublished).
- [6] G. M. Watson *et al.*, Physica (Amsterdam) **221B**, 405 (1996).
- [7] P. W. Palmberg, *et al.*, Phys. Rev. Lett. **21**, 682 (1968); R. E. Dewames and T. Wolfram, *ibid.* **22**, 137 (1969); R. J. Celotta *et al.*, *ibid.* **43**, 728 (1979); S. F. Alvarado *et al.*, *ibid.* **48**, 51 (1982); B. Dauth *et al.*, Surf. Sci. **189/190**, 729 (1987).
- [8] D. B. McWahn *et al.*, Phys. Rev. B **42**, 6007 (1990).
- [9] B. C. Frazer *et al.*, Phys. Rev. **140**, 1448 (1965); B. T. M. Willis and R. I. Taylor, Phys. Lett. **17**, 188 (1965).
- [10] R. Feidenhans'l, Surf. Sci. Rep. **10**, 105 (1989).
- [11] G. Vineyard, Phys. Rev. B **26**, 4146 (1982).
- [12] F. Stanglmeier *et al.*, Acta Crystallogr. Sect. A **48**, 626 (1992).
- [13] H. Dosch *et al.*, Phys. Rev. Lett. **60**, 2382 (1988); H. Dosch and J. Peisl, Colloq. Phys. **50**, C7-257 (1989); H. Dosch *et al.*, Phys. Rev. B **43**, 13 172 (1991); H. Reichert *et al.*, Phys. Rev. Lett. **74**, 2006 (1995).
- [14] R. Lipowsky, Phys. Rev. Lett. **49**, 1575 (1982); R. Lipowsky and W. Speth, Phys. Rev. B **28**, 3983 (1983).
- [15] S. Dietrich, in *Phase Transitions and Critical Phenomena*, edited by C. Domb and J. L. Lebowitz (Academic, New York, 1988), Vol. 12; K. R. Mecke and S. Dietrich, Phys. Rev. B **52**, 2107 (1995).
- [16] R. Lipowsky, Ferroelectrics **73**, 69 (1987).
- [17] G. M. Watson, D. Gibbs, G. H. Lander, B. D. Gaulin, H. J. Matzke, L. E. Berman, and W. Ellis (unpublished).
- [18] S. Ferrer, P. Fajardo, F. de Bergevin, J. Alvarez, X. Torrelles, H. A. van der Vegt, and V. H. Etgens, preceding Letter, Phys. Rev. Lett. **77**, 747 (1996).